On the relationship between distance information derived from cross-linking and from resonance energy transfer, with specific reference to sites located on myosin heads

Peter D. Chantler,* Terence Tao,[‡§] and Walter F. Stafford III[‡§]

*Department of Anatomy and Neuroscience, Medical College of Pennsylvania, Philadelphia PA 19129; [‡] Department of Muscle Research, Boston Biomedical Research Institute, Boston, Massachusetts 02114; and [§]Department of Neurology, Harvard Medical School, Boston, Massachusetts USA

ABSTRACT The techniques of fluorescence resonance energy transfer (FRET) and cross-linking can provide complementary information concerning the relative separation of a pair of sites. Cross-linking experiments provide an assessment of the distance of closest approach between a pair of sites. FRET measurements, by contrast, yield information about the average distance between the pair of sites. We have taken advantage of hybrid myosins to understand the relationship between distances obtained for a pair of equivalent sites, one on each myosin head, using both FRET (steady-state and time-decay) and cross-linking techniques. The rigid cross-linker, 4-4′-dimaleimidyl-stilbene-2-2′-disulfonic acid (DMSDS), can efficiently cross-link the two myosin regulatory light-chains, each at residue Cys50 of the *Mercenaria* regulatory light chain (Chantler, P. D., and S. M. Bower. 1988. *J. Biol. Chem.* 263:938–944.), indicating that these sites can come within 18 ± 2 Å of each other. In a complementary set of experiments, steady-state and time-decay measurements using fluorescence donor/acceptor pairs located at these same sites indicate transfer efficiencies of somewhat <20%, suggesting an average separation of >50 Å between sites (Chantler, P. D., and T. Tao. 1986. *J. Mol. Biol.* 192:87–99). Here, we present theoretical calculations which show that efficient cross-linking can be achieved readily in dynamic systems such as the heads of myosin, even though the necessary subpopulation of proximate molecules at any instant may be below the detection limits of time-decay-FRET. Therefore, cross-linking experiments can provide important ancillary information about the extent of motions within a marcomolecular system when used in conjunction with FRET. As a corollary, demonstration of extensive cross-linking does not necessarily indicate a static proximity; the mean separation distance should be ascertained by other methods such as FRET.

INTRODUCTION

In recent years resonance energy transfer and cross-linking have become increasingly popular techniques for deriving distance information between pairs of defined sites in macromolecular systems. In the static case, they represent independent methods of measuring a fixed distance. In the dynamic case, the relationship is not so obvious. In practice, the two techniques have appeared to not always provide independent measurements of the same separation distance. For example, fluorescence resonance energy transfer (FRET)[1] yielded a distance of 27–40 Å between the reactive sulfhydryls (SH1 and SH2) in myosin S1, (Dalbey et al., 1983; Cheung et al., 1983, 1985), yet the two sulfhydryls can be cross-linked by a disulfide bond of 2 Å (Wells and Yount, 1980) and by other cross-linkers (<10 Å) (Wells and Yount, 1980; Burke and Reisler, 1977). The same applies to the distance between Cys98 in troponin-C and Cys133 in troponin-I in the ternary troponin complex; the two sulfhydryls can be cross-linked by a variety of cross-linkers (Dobrovol'sky et al., 1984; Park et al., 1988) including a disulfide bond (Park et al., 1988) whereas FRET yields an average distance of 35–41 Å (Tao et al., 1989). A more dramatic case is the distance between a pair of equivalent sites on the two heads of myosin. In this case, probes were attached to Cys50 of *Mercenaria* regulatory light chain reconstituted with desensitized scallop myosin. FRET measurements indicate that the two translationally equivalent sites remained on average >50 Å apart from each other (Chantler and Tao, 1986): yet, cross-linking studies showed that the same two residues could be joined together by an 18 ± 2 Å bridge with high efficiency (Chantler and Bower, 1988).

To resolve these apparent discrepancies between cross-linking and FRET studies, various workers have invoked the dynamic nature of proteins. The hypothesis being that if those protein segments that contain probe-labeled residues can undergo some degree of segmental motion, then the sulfhydryls can come close to each other sufficiently frequently to achieve observable cross-linking over a period of time, while the average distance between them remains relatively large as revealed by FRET. Although such a hypothesis appears to be qualitatively reasonable, quantitative analysis of the proposal has been lacking, in part because necessary

Address correspondence to Dr. Peter D. Chantler, Department of Anatomy and Neuroscience, Medical College of Pennsylvania, 3200 Henry Avenue, Philadelphia, PA 19129.

[1] *Abbreviations used in this paper:* DMSDS, 4-4′-dimaleimidyl-stilbene-2-2′-disulfonic acid; FRET, fluorescence resonance energy transfer.

0006-3495/91/06/1242/09 $2.00

information on the geometry and extent of flexibility of the protein regions involved is seldom available.

Distance measurements between the heads of myosin may be an exception because in this case the probe locations are known to be at a pair of translationally equivalent Cys residues (so called because the location of Cys residues on the light chains of each myosin head will be at equivalent sites in the primary structure of the light chain and, therefore, would be the same distance from the head-to-neck junction), and the heads are known to possess virtually complete segmental flexibility with respect to each other (Mendelson et al., 1973; Thomas et al., 1975; Walker et al., 1985). Using certain simplifying assumptions, we have devised a model for the myosin system that allowed us to calculate simultaneously the energy transfer efficiency and the rate of cross-linking between such a pair of sites. Both quantities were found to be strongly dependent on the distance, L, between the cysteine residue and the head–neck junction of myosin, the dependence being that both decrease with increasing L. However, owing to the inverse sixth power dependence of transfer efficiency on distance, the decrease with L for transfer efficiency is much more pronounced than that for the cross-linking rate. When these calculations were applied with specific reference to our previous FRET (Chantler and Tao, 1986) and cross-linking (Chantler and Bower, 1988) studies using Cys50 of *Mercenaria* regulatory light chain, we found that at L values of 36 Å $< L <$ 48 Å, less than ~0.5% of the population of myosin molecules are so disposed that the pairs of probe attachment sites are within cross-linking distance at any instant, giving rise to an energy transfer yield that is consistent with the observed average distance of ~50–60 Å. At the same time, the kinetic analysis shows that this small proportion of myosin molecules with proximate cysteines can adequately account for the observed rate and efficiency of cross-linking of the two sites by the bismaleimidyl cross-linker, 4-4'-dimaleimidyl-stibene-2-2'-disulfonic acid (DMSDS). A preliminary account of these results has been presented (Chantler et al., 1988).

RESULTS AND DISCUSSION

The purpose of this analysis is to devise a theoretical model that allows us to predict (*a*) the efficiency of energy transfer between probes attached at two translationally equivalent sites, one on each head of myosin and (*b*) the rate of cross-linking between these two sites by homobifunctional reagents. As far as possible, the modeling results will be applied to previously obtained FRET and DMSDS cross-linking results. We begin with a discussion and analysis of energy transfer between two independently mobile sites which are tethered at a common point. Results of this analysis will be used in the discussion of cross-linking between the same two sites.

We wish to determine the distribution of the instantaneous distances between probes on the two heads of myosin and thereby predict the expected degree of energy transfer. We have chosen to represent a single myosin head with a simple model consisting of two cones sharing a base of diameter 60 Å (Fig. 1 *a*); the first, proximal cone, whose vertex is located at the head, neck junction, has an altitude of 100 Å. The second cone, meant to represent the distal portion of the head, has an altitude of ~60–90 Å. The magnitude of the altitude of the distal cone is not important for this analysis. These dimensions are consistent with electron microscopic observations (Milligan and Flicker, 1987). A vector, **S**, drawn along the side of the cone to join the vertex to the widest point, would subtend an angle of arctan (30 Å/100 Å) = 16.7° with the head axis **A**, see Fig. 1 *a*. The length of **S** would be greater than the length of **L**, the vector drawn from the head, neck junction to the Cys50 residue on the light chain. Now, consider the following model of myosin (Fig. 1 *b*) in which the swivel point between the two heads is connected to the probes (located at the same distance, L, from the swivel on each head) by vectors $\mathbf{L}_1$ and $\mathbf{L}_2$. In this model the axis of the first head ($\mathbf{A}_1$) is made to coincide with the z-axis whereas the axis of the second head ($\mathbf{A}_2$) is allowed freely independent motion. Let θ be the angle between $\mathbf{A}_1$ and $\mathbf{A}_2$. The vectors $\mathbf{L}_1$ and $\mathbf{L}_2$, would subtend the same angle, 16.7°, with $\mathbf{A}_1$ and $\mathbf{A}_2$, respectively. Therefore, the angle of closest approach of the head axes (i.e., the angle at which the heads would just touch at the widest part), $\theta_{1,\min}$, would be just twice this angle and equal to 33.4°. At first we will allow only a rotational motion in the y–z plane about the x-axis by angle θ to make the development conceptually simpler; later, the restriction will be removed to include rotation around the z-axis as well. In this orientation, each head is allowed to rotate around its own axis by angles α_1 and α_2, respectively (Fig. 1 *b* and Fig. 2), so that the vectors $\mathbf{L}_1$ and $\mathbf{L}_2$ trace out the circular locus of the Cys50 residues as each head rotates about its own axis, $\mathbf{A}_i$. In this model, the myosin tail is allowed to have completely free motion and is assumed not to interfere with motion of the heads.

The instantaneous distance between the probes is given by $\mathbf{R} = \mathbf{L}_2 - \mathbf{L}_1$. For the first head, referring to Fig. 1 *b*, we can write that:

$$\mathbf{L}_1 = [r \cos(\alpha_1)]\mathbf{i} + [r \sin(\alpha_1)]\mathbf{j} + [A]\mathbf{k},$$

where r is the radius of the circle perpendicular to and

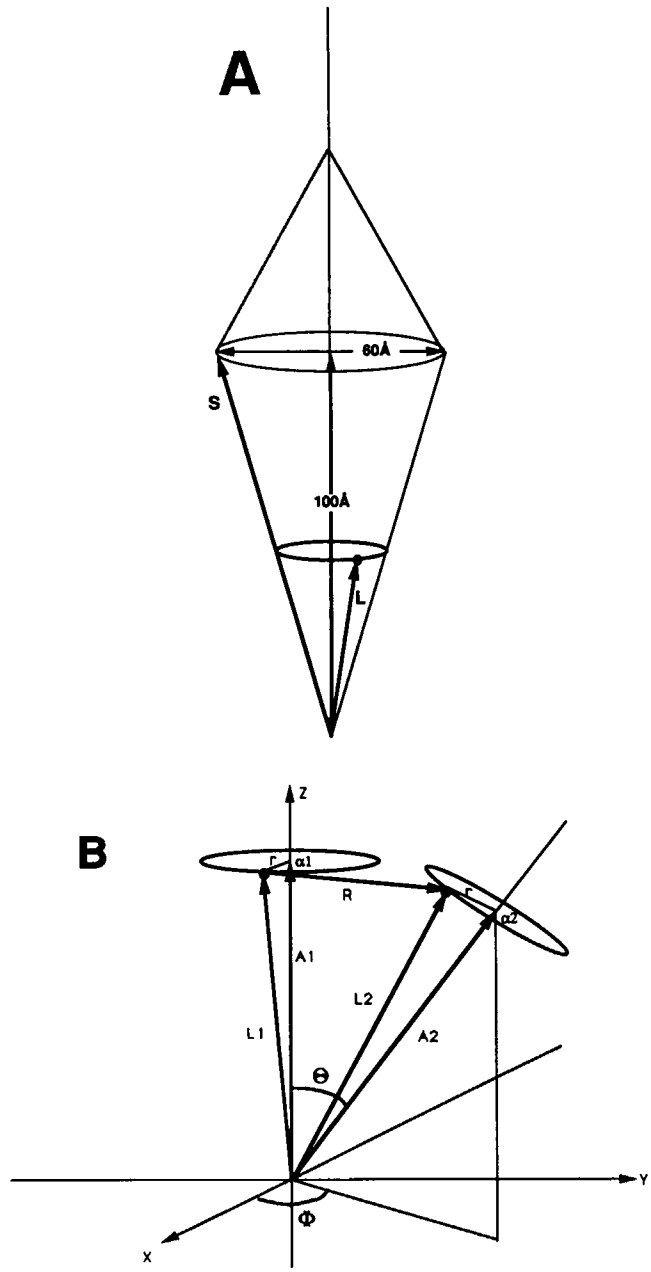

FIGURE 1 (*A*) Simplified conical model of the myosin head showing the specific geometry used in the calculations and showing the envisaged relation of the probe location to the overall head geometry. (*B*) Diagram showing the coordinate system and the location of the probes at the ends of vectors $\mathbf{L}_1$ and $\mathbf{L}_2$, respectively. θ is the angle between the head axes, $\mathbf{A}_1$ and $\mathbf{A}_2$. The head axes cannot approach any closer than $\theta_{min} = 2 \arctan (30 \text{ Å}/100 \text{ Å})$. In the text, we have defined an angle, β, of closest approach of the probes so that $\beta = 0$ when $\theta = \theta_{min}$. The geometry requires that $0 \leq \beta \leq 147°$. The heads are allowed to rotate about their axes through angles $0 \leq \alpha_1 \leq 2\pi$, and $0 \leq \alpha_2 \leq 2\pi$. $\mathbf{R}$ is a vector joining the probes and its magnitude, R, gives the instantaneous distance between the probes. The other parameters are explained in the text.

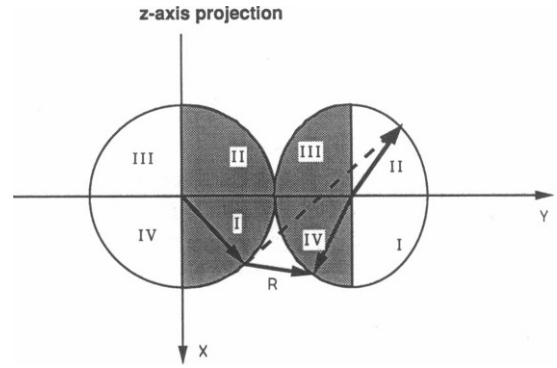

FIGURE 2 A *z*-axis projection of the circular loci of the probes to show that distances corresponding to only those orientations of the probes which were on facing sides of the heads were counted as cross-linkable distances. Cross-linking through the heads (represented by the *dashed vector*) was eliminated by this restriction. Distances between sector I on the left head and sector III on the right head, for example, were allowed by assuming limited flexibility of the probe and/or residues on the heads with which they could react. This approximation will not seriously affect the result.

centered on the head axis $\mathbf{A}_1$, A is the length of $\mathbf{A}_1$ from the head–neck junction to the level of the probe, and α_1 is the angular position of the probe measured with respect to an arbitrary reference radius vector perpendicular to the head axis vector $\mathbf{A}_1$.

The components of $\mathbf{L}_2$, given by rotation of $\mathbf{L}_1$ about the *x*-axis by angle θ, are obtained by applying rotation operator $\mathbf{R}_x$ to $\mathbf{L}_1$ such that $\mathbf{L}_2 = \mathbf{R}_x\mathbf{L}_1$:

$$\begin{pmatrix} r\cos(\alpha_2) \\ r\cos(\theta)\sin(\alpha_2) + A\sin(\theta) \\ -r\sin(\theta)\sin(\alpha_2) + A\cos(\theta) \end{pmatrix} = \begin{pmatrix} 1 & 0 & 0 \\ 0 & \cos(\theta) & \sin(\theta) \\ 0 & -\sin(\theta) & \cos(\theta) \end{pmatrix} \begin{pmatrix} r\cos(\alpha_1) \\ r\sin(\alpha_1) \\ A \end{pmatrix}.$$

Therefore,

$$\mathbf{L}_2 = [r\cos(\alpha_2)]\mathbf{i} + [r\cos(\theta)\sin(\alpha_2) + A\sin(\theta)]\mathbf{j} + [-r\sin(\theta)\sin(\alpha_2) + A\cos(\theta)]\mathbf{k},$$

where r, A, and α_2 have the same meaning as for the first circle. Finally, the instantaneous distance, $R(\theta, \alpha_1, \alpha_2)$, between the two probes is given by

$$R(\theta, \alpha_1, \alpha_2) = \{r^2[\cos(\alpha_2) - \cos(\alpha_1)]^2 + [r\cos(\theta)\sin(\alpha_2) + A\sin(\theta) - r\sin(\alpha_1)]^2 + [-r\sin(\theta)\sin(\alpha_2) + A\cos(\theta) - A]^2\}^{1/2},$$

and the instantaneous energy transfer efficiency, $E(\theta, \alpha_1, \alpha_2)$, is given by

$$E(\theta, \alpha_1, \alpha_2) = \frac{1}{(1 + [R(\theta, \alpha_1, \alpha_2)/R_0)^6]},$$

where R_0 is called the critical transfer distance and corresponds to the distance at which the efficiency is equal to 0.5 (Förster, 1948). Now, at a particular value of $\theta = \theta'$, the average distance, $\langle R(\theta') \rangle$, between the probes is given by integration over all angular orientations ($0 \leq \alpha_1 \leq 2\pi$, and $0 \leq \alpha_2 \leq 2\pi$) of the heads about their respective axes $\mathbf{A}_1$ and $\mathbf{A}_2$,

$$\langle R(\theta') \rangle = \frac{1}{4\pi^2} \int_{\alpha_1=0}^{2\pi} \int_{\alpha_2=0}^{2\pi} R(\theta', \alpha_1, \alpha_2) \, d\alpha_1 \, d\alpha_2.$$

Likewise, the average efficiency, $\langle E(\theta') \rangle$, at the same value of $\theta = \theta'$ is given by

$$\langle E(\theta') \rangle = \frac{1}{4\pi^2} \int_{\alpha_1=0}^{2\pi} \int_{\alpha_2=0}^{2\pi} E(\theta', \alpha_1, \alpha_2) \, d\alpha_1 \, d\alpha_2.$$

For any given value of $\theta = \theta'$, the value of both $\langle R(\theta') \rangle$ and $\langle E(\theta') \rangle$ is independent of ϕ ($0 \leq \phi \leq 2\pi$); therefore, it is not necessary to repeat the integration over ϕ, and so the restriction above to the y–z plane can be removed.

Because we are allowing unrestricted motion of $\mathbf{A}_2$ within the allowed angular limits of θ, it is equally likely that the tip of $\mathbf{A}_2$ will be found within any surface element of arbitrary size within those limits. Therefore, the probability density function, $dP(\theta)/d\theta$, of θ can be shown to be given by

$$\frac{dP(\theta)}{d\theta} = K \sin \theta,$$

and if θ is limited to $0 \leq \theta_1 \leq \theta \leq \theta_2 \leq \pi$, the normalization constant, K, is given by

$$K = \frac{1}{\int_{\theta_1}^{\theta_2} \sin \theta \, d\theta} = \frac{1}{\cos \theta_1 - \cos \theta_2},$$

so that

$$\frac{dP(\theta)}{d\theta} = \frac{\sin \theta}{\cos \theta_1 - \cos \theta_2}.$$

Dropping the angle brackets above on $\langle R(\theta') \rangle$ and remembering that it has been averaged already over α_1 and α_2 at each value of θ, the average value of $R(\theta)$, $\langle R \rangle$, over the range, $\theta_1 \leq \theta \leq \theta_2$, is given by

$$\langle R \rangle = \int_{\theta_1}^{\theta_2} R(\theta) \frac{dP(\theta)}{d\theta} \, d\theta = \frac{1}{(\cos(\theta_1) - \cos(\theta_2))} \int_{\theta_1}^{\theta_2} R(\theta) \sin(\theta) \, d\theta.$$

Similarly, again dropping the angle brackets and remembering that $\langle E(\theta') \rangle$ has been averaged already over α_1 and α_2 at each value of θ, the average value of the energy transfer efficiency, $E(\theta)$, is given by

$$\langle E \rangle = \int_{\theta_1}^{\theta_2} E(\theta) \frac{dP(\theta)}{d\theta} \, d\theta = \frac{1}{(\cos(\theta_1) - \cos(\theta_2))} \int_{\theta_1}^{\theta_2} E(\theta) \sin(\theta) \, d\theta.$$

The numerical integration of these relations was carried out by the trapezoidal rule in one degree increments over a specified range of θ for various values of L for a given R_0. A set of curves showing the values of the average efficiency as a function of L for various values for the angle of closest approach of the probes with $\theta_2 = \pi$, is shown in Fig. 3. For convenience, we will define β as the angle of closest approach between the probes, $\mathbf{L}_1$ and $\mathbf{L}_2$ so that when $\theta_1 = \theta_{1,\min}$, $\beta = 0$.

The curve for $\beta = 0°$ in Fig. 3 is shown as one extreme case in which there would be no restriction preventing

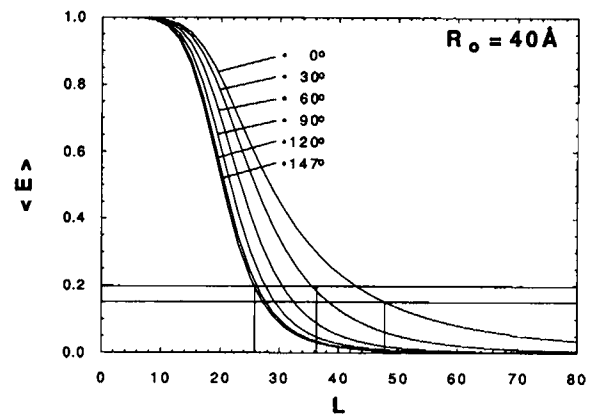

FIGURE 3 The efficiency of energy transfer (y-axis) averaged over all possible orientations of the fluorescence probes attached to equivalent positions on the myosin heads. The curves correspond to the indicated angle, β, of closest approach of the probes to each other. The x-axis is the distance, L, from the head–tail junction to the probe. If the x-axis were normalized by dividing by R_0, this curve would be completely general and could be used with a probe of any value of R_0. Therefore, this curve could be used to choose a probe so that it could give the maximum amount of information about the limits of L (see Discussion).

the probes from coming into contact; the curve for $\beta = 147°$ is the other extreme case for which heads would always be fully extended. Although these extreme cases may be unrealistic, they put upper and lower limits on the amount of energy transfer that could be expected for this type of system. The companion curves, for several intermediate values of β, were considered in order to address the likely situation of steric hindrance as the heads approached each other. This could arise for several possible reasons. There might be protuberances near the head neck junction that could interact before the heads came into contact at the widest point causing β to be significantly larger than zero. Alternatively, the surface of the head, and therefore the probe, might lie within the proximal cone so that β would be larger than zero when the heads were touching at their widest point. These possibilities were considered and treated by examining what happens to the value of $\langle E \rangle$ as β increased from zero to its maximum possible value of 147° (Fig. 3).

At this point the analysis is completely general for a system of this geometry. There are several features of the curves in Fig. 3 that are worth pointing out. For any measured value of $\langle E \rangle$ with its uncertainty of $\pm\delta\langle E \rangle$, one may use Fig. 3 or a similarly derived set of curves to set limits on L. At the higher values of $\langle E \rangle$ the possible range of L becomes fairly narrow and practically independent of any restrictions on the motion. At lower values of $\langle E \rangle$, the set of curves may be used to set a lower limit on the value of L. For example, in the case we are considering here, the observed energy transfer efficiency was in the range of 15–20%. In Fig. 3, a horizontal line is shown at each of these values. The upper limit for L is obtained from the point at which the lower line, at $\langle E \rangle - \delta\langle E \rangle$, intersects the curve for $\beta = 0°$. The extreme lower limit for L is obtained from the point at which the upper line, at $\langle E \rangle + \delta\langle E \rangle$, intersects the curve for $\beta = 147°$. Therefore, without taking the cross-linking results into account, the possible range for L would be from 25 to 48 Å. As will be discussed below, the cross-linking results will put further restrictions on the lower limit of L.

Obviously, there are values of β for which no cross-linking would be possible. If one considers a cross-linker located a distance L from the head neck junction then a simple geometrical argument shows that the cross-linking distance between the Cys50 residues is given by $R = 2L \sin(\beta/2)$, where β, as defined above, is the angle between $\mathbf{L}_1$ and $\mathbf{L}_2$ at their closest approach. Values of β larger than $\beta_{max} = 2 \arcsin(R_{XL}/2L)$, where R_{XL} is the length of a particular cross-linker, would preclude cross-linking. Therefore, the upper limit for β, β_{max}, and the lower limit for L, L_{min}, must be consistent with each other. The values of β and L_{min} consistent with β_{max} are found in the following way (Fig. 4): for each curve in Fig. 3 corresponding to a particular value of β, the value of L at the intersection with the horizontal line at $\langle E \rangle = 0.2$ is equal to L_{min}. This value of L_{min} is used to calculate the corresponding value of β_{max}, using the above equation. These pairs of values of β and β_{max} are plotted against each other along with a plot of the straight line $\beta = \beta_{max}$. The correct value of β_{max} is obtained from the intersection of these two plots. For the particular situation we are considering here (using $\langle E \rangle = 0.2$, $R = 18$ Å), the upper limit for β would be ~29°. The graphical method just described gives a value 36 Å for the lower limit of L, Fig. 4 *b*, whereas the curve for $\beta = 0$ gives a value 48 Å for the upper limit. Thus, the cross-linking results have allowed us to restrict the range of L even further to 36 Å $< L <$ 48 Å. A value of L in this range is in

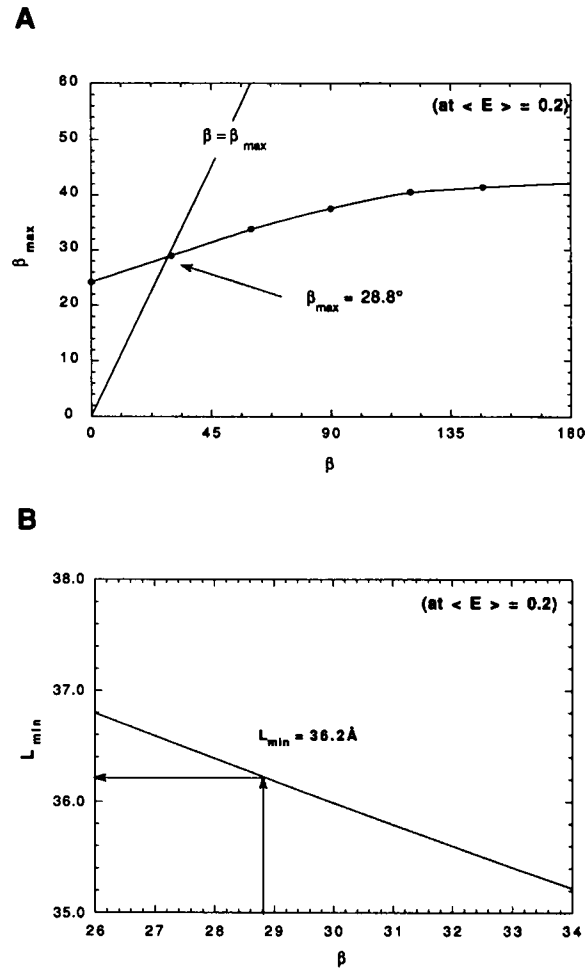

FIGURE 4 (*A*) (*a*) Plot of β versus β_{max} obtained from the values of L_{min} corresponding to $\langle E \rangle = 0.2$ from intersection with the curve at each value of β. (*b*) Plot of $\beta = \beta_{max}$. The intersection of these two plots gives the maximum value of β that satisfies the requirements of both the energy transfer results and the cross-linking results. (*B*) Plot of L_{min} versus β from which the corresponding value of L_{min} is obtained.

reasonable agreement with the electron microscope (EM) observations (15 Å < L < 35 Å) of Chantler and Kensler (1989) because EM measurements suffer from the problem of foreshortening and, in general, are probably no more accurate than ±20 Å. Moreover, the conclusion that β is <30° indicates that the motion of the heads is probably not severely restricted.

Now we are ready to consider the *a priori* estimation of cross-linking rates. Cross-linking between the heads is viewed as a two step process: a collision followed by a chemical reaction (Fig. 5). The first step is governed by the collision constant, k_d. The ability of the cross-linker, already attached to the Cys50 site on one myosin head, to interact with Cys50 on the other myosin head will be controlled, in part, by the rate of diffusion of the two tethered heads. The second step may be rate-limiting, for when the two "reactive patches" (i.e., the area on the surface of the protein within which each reactive ligand can rotate on its side chain) on each myosin head come together, they will "hover" near each other for a long period of time compared with the time taken for a successful collision to become committed to cross-linking (rate k_{XL}). Alternatively, a rapid attachment–detachment equilibrium may occur which has on–off rates much faster than the subsequent steps of the cross-linking mechanism. In Fig. 5, this would be accommodated by the reverse arrow labeled k_r having a rate constant comparable to k_d.

First, we develop the theory for the case with completely free motion of the heads within the volume defined by their range of relative motion. The diffusion-controlled rate constant for a bimolecular reaction between separate globular molecules is given by:

$$k_d = \frac{4\pi N}{10^3} r_{12} D_{12},$$

where N is Avogadro's number (6.023×10^{23} mol^{-1}); r_{12} is the sum of the two effective radii (Alberty and Hammes, 1958); and D_{12} is the sum of the diffusion coefficients of the two molecules. Using the Stokes–Einstein and Svedberg relationships (Tanford, 1961), a molecular weight of 115,000 D and a sedimentation coefficient of 5.8S for free S-1 (Lowey et al., 1969), we calculate the effective (Stokes) radius to be 48 Å giving $r_{12} = 96$ Å $= 96 \times 10^{-8}$ cm and $D_{12} = 9.4 \times 10^{-7}$ cm$^2 \times$ s^{-1}. Inserting the values for free S-1, we obtain $k_d = 6.8 \times 10^9$ M$^{-1} \times$ s^{-1}.

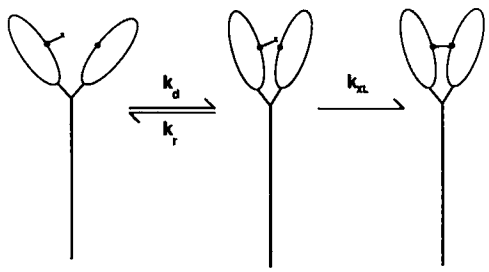

FIGURE 5 The cross-linking reaction is viewed as a two step process governed in the forward direction by the rate of diffusional collision of the two heads, k_d, and by the rate of the chemical cross-linking reaction, k_{XL}. The first step is also considered to be reversible with a rate, k_r, comparable to the collision rate.

Simplifying assumptions made in obtaining this value now need to be addressed. In our case the two S-1 heads are not free but are tethered together as the two heads of myosin. Also, as the cross-linking reaction is intramolecular, it should be independent of the overall myosin concentration. By using a calculated effective concentration for the tethered heads, we can convert k_d to a pseudo-first order rate constant $k_{d,eff}$. To obtain the effective head concentration, assume the two heads are constrained within a sphere of radius 130 Å (maximum chord of S-1; value obtained from Milligan and Flicker, 1987). This gives an effective head concentration of $[S\text{-}1]_{eff} = 3.6 \times 10^{-4}$ M. Multiplying k_d by this value, we get an estimate of the maximum effective pseudo-first order rate constant of $\sim k_{d,eff} = k_d[S\text{-}1]_{eff} = 2.4 \times 10^6$ s^{-1}.

This estimated rate constant will have to be decreased further because there will be a certain probability that each of the reactive patches are in the appropriate orientation for the reaction to proceed. This probability can be broken down into two components. The closer the cross-linker is situated to the head neck junction along the head axis of Fig. 1, the higher its probability of cross-linking because a smaller diffusion distance will get it within cross-linking range. The range of L to consider, in light of the above discussion on the relationship of L to energy transfer efficiency, is 36–48 Å. The probability density function of R, $p(R)$, is needed for a discussion of the cross-linking experiments so that one can estimate the fraction of molecules that would be expected to be within cross-linking distance and orientation at any one time. In the calculation described above, the probability density function was numerically computed by counting each calculated distance that fell within 1 Å intervals. Plots of $p(R)$ versus R for the two extreme cases (L = 36 Å; β = 29° and L = 48 Å; β = 0°) with $\theta_2 = \pi$ are shown in curve *a* of Fig. 6, *A* and *B*, respectively. The probability of cross-linking was estimated with the added restriction that cross-linking can occur only between Cys50 residues that are in favorable orientations, shown in curve *b* (Fig. 6, *A* and *B*) (i.e., cross-linking through the S-1 head is not permitted; see Fig. 2). The area under the curves in Fig. 6 for 16 Å < R < 20 Å gives the probability of cross-linking for the chosen values of R and L for DMSDS. Choosing L = 36 Å and β = 29°, the probability of cross-linking is $\sim 5.0 \times 10^{-4}$. For L = 48 Å and β = 0°, the probability of

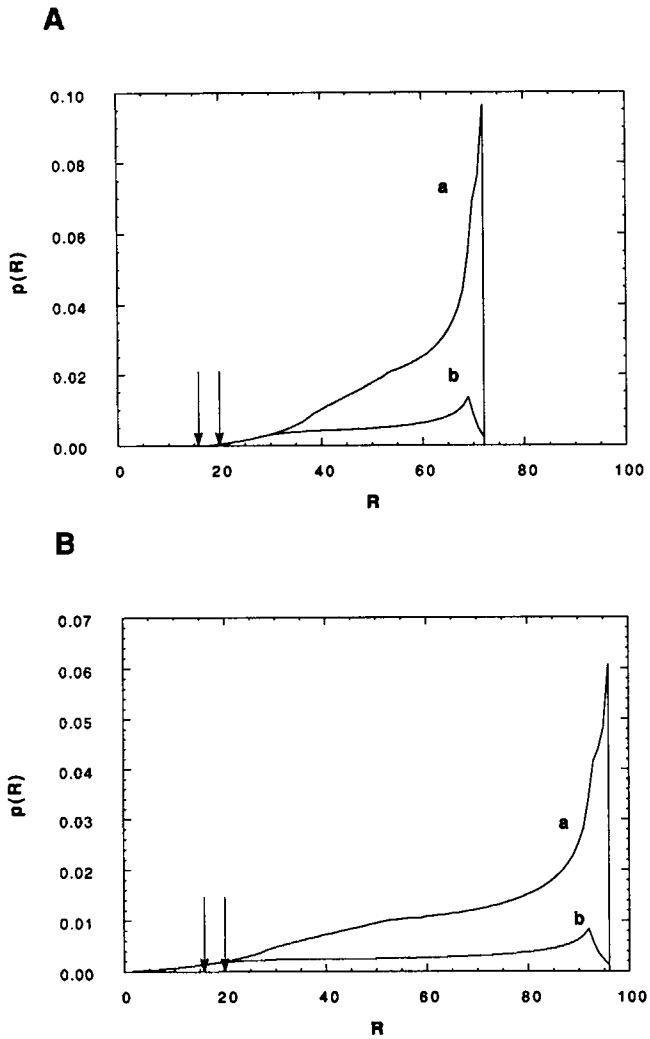

FIGURE 6 The differential probability distribution function of the normalized distances between the probes is shown for two cases; (*A*) Curve *a*: the distance distribution was calculated for $L = 36$ Å with $\beta = 29°$. Curve *b* includes only those distances from curve a that are between cross-linkable sites as defined in the text (See Fig. 2). (*B*) Curve *a* was calculated for $L = 48$ Å with $\beta = 0°$. Curve *b* includes only the cross-linkable fraction of those shown in curve *a*. The indicated area under the curves, between the arrows, gives the probability, p (16 Å $< L <$ 20 Å), that a distance will fall between 16 and 20 Å.

cross-linking is $\sim 8.0 \times 10^{-3}$. Choosing an intermediate value of 4×10^{-3}, this gives a calculated value of the effective pseudo-first order rate constant of $k_{\text{eff,d,calc}} = (2.4 \times 10^6\ \text{s}^{-1})\ (4.0 \times 10^{-3}) = 9.6 \times 10^3\ \text{s}^{-1}$. At the same time, the average distance between the probes would be $\langle R \rangle = 55$ Å assuming $L = 36$ Å and $\beta = 29°$; and $\langle R \rangle = 67$ Å assuming $L = 48$ Å and $\beta = 0°$.

The above calculations determine the theoretical rate of entry into the reaction; any estimate of the actual rate requires an estimate of k_{XL}, the rate constant of the chemical cross-linking reaction. The maleimidyl modification of sulfhydryl groups is a relatively slow reaction; even at pH 7.0, the rate constant is $\sim 750\ \text{M}^{-1}\ \text{s}^{-1}$ (Gregory, 1955; Smyth et al., 1960; Means and Feeley, 1971). This rate constant is less than our theoretical, diffusion-limited second order reaction rate constant by a factor of the order of 10^7. Using our estimate of the probability of Cys50 residues being in cross-linking orientation ($5 \times 10^{-4} < p < 8 \times 10^{-3}$) and multiplying it by the effective head concentration (3.6×10^{-4} M) and by the rate constant for reaction of maleimidyl modification of sulfhydryls, we estimate a first order rate constant between 1.4×10^{-4} and $2.2 \times 10^{-3}\ \text{s}^{-1}$. The rate constant we observed experimentally for the DMSDS cross-linking reaction was $2 \times 10^{-3}\ \text{s}^{-1}$. Our rough estimates are very close to what was actually observed. Therefore, we would expect efficient cross-linking even for our restricted model with $\beta = 29°$.

Our calculations here show that there is a region for the location of Cys50 of the *Mercenaria* regulatory light-chain, 36–48 Å from the head neck junction, where theory, cross-linking data and FRET data are mutually compatible. One notable aspect of our results is their dependence on L. Both the efficiency of energy transfer and the efficiency of cross-linking are predicted to increase as the distance, L, from the head neck junction to the probe decreases. Our model is likely to be least realistic, and therefore least accurate, at low value of L, where the two heads approach the neck of myosin. In this region, where all six myosin polypeptides come together, the light-chains may assume a more globular configuration, thus adding to the mass and thereby, the excluded volume, in this region. The lower end of the range for L falls close to the upper limit of L values (viz. 15–35 Å) deduced from electron microscopic localization of Cys50 using biotin-avidin labeled *Mercenaria* regulatory light chain (Chantler and Kensler, 1989). However, because of possible foreshortening in the EM, the upper limit obtained from EM measurements is probably closer to the true distance from the head neck junction than the lower end of the range. Thus, our present work highlights the internal consistency between all three sets of distance determinations, and provides a quantitative basis for the interpretation of cross-linking and energy transfer results in dynamic systems. The foregoing analysis clearly shows that there is no necessary conflict between a high efficiency of cross-linking and a low efficiency of energy transfer, in a situation where probes are placed on constrained yet otherwise independently mobile sites, as on each of the two heads of myosin.

When FRET data are used to establish limits on L, as in Fig. 3, it is assumed that the efficiency of energy transfer has been determined correctly in the sense that

a suitable value for κ^2, the orientation factor, has been selected. The problem of choosing a correct value of κ^2 has been much discussed in the literature, and a number of statistical treatments are available (Hillel and Wu, 1976; Stryer, 1978). As noted by Perkins et al. (1984), because proteins undergo considerable structural fluctuations on a picosecond time scale, it is unlikely that significant errors will be introduced by choosing a value of $\kappa^2 = 2/3$, corresponding to an isotropic distribution of dipole moments. In the case of the specific results described here, the practical and theoretical considerations which led us to choose a value of $\kappa^2 = 2/3$ in our calculations have been outlined in detail elsewhere (Chantler and Tao, 1986).

Assuming that correctly determined values of the efficiency are available (i.e., the correct value of κ^2 has been used), the curves presented in Fig. 3 can be used for any system of similar geometry. For example, if the x-axis were normalized by dividing by R_0, then these curves could be used with any donor–acceptor pair. If one were to chose a donor–acceptor pair with a value of R_0 such that the value of $\langle E \rangle$ was about 0.7–0.9, then a fairly narrow range for the estimate of L could be obtained without regard to steric hindrance. Alternatively, these curves could be used to get an idea of the amount of steric hindrance experienced by the domains to which the probes were attached. For example, if the value of L were known, then a donor–acceptor pair with a value of R_0 could be chosen in the neighborhood of $L/R_0 = 0.75$ to give values of $\langle E \rangle$ from 0.1 to 0.4. Values of $\langle E \rangle < 0.4$ would indicate that motion was restricted. The methods presented here could be extended easily to systems of other geometry by rephrasing the model and generating the appropriate vectorial relationships.

We thank Dr. John Gergley for critical reading of the manuscript, and we thank Miss Susanne Bower for expert technical assistance.

This work was performed during the tenure of grants from the American Heart Association (870688), National Science Foundation (DMB-8602246), National Institutes of Health (AR-32858) to Peter D. Chantler; from National Institutes of Health (AR-21673) to Terence Tao and National Institutes of Health (RR-05711) to B.B.R.I.

Received for publication 13 August 1990 and in final form 28 January 1991.

REFERENCES

Alberty, K. A., and G. G. Hammes. 1958. Application of the theory of diffusion-controlled reactions to enzyme kinetics. *J. Phys. Chem.* 62:154–159.

Burke, M., and E. Reisler. 1977. Effect of nucleotide binding on the proximity of the essential sulfhydryl groups of myosin. Chemical probing of movement of residues during conformational transitions. *Biochemistry.* 16:5559–5563.

Chantler, P. D., and S. M. Bower. 1988. Cross-linking between translationally equivalent sites on the two heads of myosin. Relationship to energy transfer results between the same pair of sites. *J. Biol. Chem.* 263:938–944.

Chantler, P. D., and R. W. Kensler. 1989. Position of *Mercenaria* regulatory light-chain Cys-50 site on the surface of myosin visualized by electron microscopy. *J. Mol. Biol.* 207:631–636.

Chantler, P. D., and T. Tao. 1986. Interhead fluorescence energy transfer between probes attached to translationally equivalent sites on the regulatory light-chains of scallop myosin. *J. Mol. Biol.* 192:87–99.

Chantler, P. D., S. M. Bower, T. Tao, and W. F. Stafford. 1988. The combined use of FRET and cross-linking to estimate distances between mobile sites. *Biophys. J.* 53:293*a*. (Abstr.)

Cheung, H. C., F. Gonsoulin, and F. Garland. 1983. Fluorescence energy transfer studies on the proximity of the two essential thiols of myosin subfragment-1. *J. Biol. Chem.* 258:5775–5786.

Cheung, H. C., F. Gonsoulin, and F. Garland. 1985. An investigation of the SH_1–SH_2 and SH_1–ATPase distances in myosin subfragment-1 by resonance energy transfer using nanosecond fluorimetry. *Biochim. Biophys. Acta.* 832:52–62.

Dalbey, R. E., J. Weiel, and R. G. Yount. 1983. Förster energy transfer measurements of thiol 1 to thiol 2 distances in myosin subfragment-1. *Biochemistry.* 22:4696–4706.

Dobrovol'sky, A. B., N. B. Gusev, and P. Friedrich. 1984. Crosslinking of troponin complex with 1,3-Difluoro-4,6-Dinitrobenzene. Identification of the crosslink formed between troponin C and troponin I in the absence of Ca^{2+}. *Biochim. Biophys. Acta.* 789:144–151.

Förster, Th. 1948. Annelen der Physik. Series 6. Intermolecular Energy Migration and Fluorescence. (Translated by R. S. Knox, 1974.) University of Rochester, New York. 2:55–75.

Gregory, J. D. 1955. The stability of *N*-ethylmaleimide and its reaction with sulfhydryl groups. *J. Am. Chem. Soc.* 77:3922–3923.

Hillel, Z., and C-W. Wu. 1976. Statistical interpretation of fluorescence energy transfer measurements in macromolecular systems. *Biochemistry.* 15:2105–2113.

Lakowicz, J. R. 1983. Principles of Fluorescence Spectroscopy. Plenum Publishing Corp., New York. 303–336.

Lowey, S., H. S. Slayter, A. G. Weeds, and H. Baker. 1969. Substructure of the myosin molecule. *J. Mol. Biol.* 42:1–29.

Means, G. E., and R. E. Feeney. 1971. Chemical Modification of Proteins. Holden-Day, Inc., San Francisco, CA. 105–138.

Mendelson, R. A., M. F. Morales, and J. Botts. 1973. Segmental flexibility of the S-1 moiety of myosin. *Biochemistry.* 12:2250–2255.

Milligan, R. A., and P. F. Flicker. 1987. Structural relationships of actin, myosin and tropomyosin revealed by cryo-electron microscopy. *J. Cell Biol.* 105:29–39.

Park, H.-S., B.-J. Gong, and T. Tao. 1988. Troponin-C can be cross-linked to troponin-I by a disulfide bond. *Biophys. J.* 53:587*a*. (Abstr.)

Perkins, W. J., J. Weiel, J. Grammer, and R. G. Yount. 1984. Introduction of a donor–acceptor pair by a single protein modification. *J. Biol. Chem.* 259:8786–8793.

Smyth, D. G., A. Nagamatsu, and J. S. Fruton. 1960. Some reactions of *N*-ethylmaleimide. *J. Am. Chem. Soc.* 82:4600–4604.

Stryer, L. 1978. Fluorescence energy transfer as a spectroscopic ruler. *Annu. Rev. Biochem.* 46:819–846.

Tanford, C. 1961. Physical Chemistry of Macromolecules. John Wiley & Sons, New York.

Tao, T., E. Gowell, G. M. Strasburg, J. Gergely, and P. C. Leavis. 1989. Ca^{2+}-dependence of the distance between Cys-98 of troponin C and Cys-133 of troponin I in the ternary troponin complex. Resonance energy transfer measurements. *Biochemistry.* 28:5902–5908.

Thomas, D. D., J. C. Seidel, J. S. Hyde, and J. Gergely. 1975. Motion of subfragment-1 in myosin and its supramolecular complexes: saturation transfer electron paramagnetic resonance. *Proc. Natl. Acad. Sci. USA.* 72:1792–1733.

Walker, M., P. Knight, and J. Trinick. 1985. Negative staining of myosin molecules. *J. Mol. Biol.* 184:535–542.

Wells, J. A., and R. G. Yount. 1980. Reaction of 5,5'-Dithiobis[2-nitrobenzoic acid] with myosin subfragment one: evidence for formation of a single protein disulfide with trapping of metal nucleotide at the active site. *Biochemistry.* 19:1711–1717.